

## Augmentation of NAD<sup>+</sup> levels by enzymatic action of NAD(P)H quinone oxidoreductase 1 attenuates adriamycin-induced cardiac dysfunction in mice



Dipendra Khadka<sup>a,1</sup>, Hyung-Jin Kim<sup>a,1</sup>, Gi-Su Oh<sup>a</sup>, AiHua Shen<sup>a</sup>, SeungHoon Lee<sup>a</sup>, Su-Bin Lee<sup>a</sup>, Subham Sharma<sup>a</sup>, Seon Young Kim<sup>a</sup>, Arpana Pandit<sup>a</sup>, Seong-Kyu Choe<sup>a</sup>, Tae Hwan Kwak<sup>a</sup>, Sei-Hoon Yang<sup>b</sup>, Hyuk Sim<sup>b</sup>, Gwang Hyeon Eom<sup>c</sup>, Raekil Park<sup>d</sup>, Hong-Seob So<sup>a,\*</sup>

<sup>a</sup> Center for Metabolic Function Regulation, & Department of Microbiology, Republic of Korea.

<sup>b</sup> Internal Medicine, School of Medicine Wonkwang, University School of Medicine, Iksan, Jeonbuk 54538, Republic of Korea.

<sup>c</sup> Department of Pharmacology, Medical Research Center for Gene Regulation Chonnam, National University Medical School, Hwasungun Jeollanam-do 58128, Republic of Korea.

<sup>d</sup> Department of Biomedical Science & Engineering, Institute of Integrated Technology, Gwangju Institute of Science and Technology, Gwangju 61005, Republic of Korea.

### ARTICLE INFO

#### Keywords:

Adriamycin  
Cardiomyopathy  
Dunnione  
NQO1  
NAD<sup>+</sup>/NADH ratio

### ABSTRACT

**Background:** Adriamycin (ADR) is a powerful chemotherapeutic agent extensively used to treat various human neoplasms. However, its clinical utility is hampered due to severe adverse side effects i.e. cardiotoxicity and heart failure. ADR-induced cardiomyopathy (AIC) has been reported to be caused by myocardial damage and dysfunction through oxidative stress, DNA damage, and inflammatory responses. Nonetheless, the remedies for AIC are even not established. Therefore, we illustrate the role of NAD<sup>+</sup>/NADH modulation by NAD(P)H quinone oxidoreductase 1 (NQO1) enzymatic action on AIC.

**Methods and results:** AIC was established by intraperitoneal injection of ADR in C57BL/6 wild-type (WT) and NQO1 knockout (NQO1<sup>-/-</sup>) mice. All Mice were orally administered dunnione (named NQO1 substrate) before and after exposure to ADR. Cardiac biomarker levels in the plasma, cardiac dysfunction, oxidative biomarkers, and mRNA and protein levels of pro-inflammatory mediators were determined compared the cardiac toxicity of each experimental group. All biomarkers of Cardiac damage and oxidative stress, and mRNA levels of pro-inflammatory cytokines including cardiac dysfunction were increased in ADR-treated both WT and NQO1<sup>-/-</sup> mice. However, this increase was significantly reduced by dunnione in WT, but not in NQO1<sup>-/-</sup> mice. In addition, a decrease in SIRT1 activity due to a reduction in the NAD<sup>+</sup>/NADH ratio by PARP-1 hyperactivation was associated with AIC through increased nuclear factor (NF)-κB p65 and p53 acetylation in both WT and NQO1<sup>-/-</sup> mice. While an elevation in NAD<sup>+</sup>/NADH ratio via NQO1 enzymatic action using dunnione recovered SIRT1 activity and subsequently deacetylated NF-κB p65 and p53, however not in NQO1<sup>-/-</sup> mice, thereby attenuating AIC.

**Conclusion:** Thus, modulation of NAD<sup>+</sup>/NADH by NQO1 may be a novel therapeutic approach to prevent chemotherapy-associated heart failure, including AIC.

### 1. Introduction

Anthracyclines are the most widely available antineoplastic drugs for cancer chemotherapy [1]. Among them, adriamycin (ADR; doxorubicin), a cytotoxic chemotherapeutic drug, widely used to treat a variety of cancers, including both human solid tumors and hematological malignancies [2]. However, the cumulative dose-dependent

cardiotoxic side effects of the drug can eventually lead to serious heart failure and limit its clinical use. The pathogenic mechanisms implicated in ADR-induced cardiomyopathy may include oxidative stress induced by reactive oxygen species (ROS) production, DNA damage, induction of apoptosis, alteration of mitochondrial metabolism, calcium dysregulation [3], and inflammation [4], which lead to cardiac remodeling and dysfunction. In ADR-induced cardiotoxicity, oxidative stress

\* Corresponding author at: Department of Microbiology, Wonkwang University School of Medicine, 460 Iksan-Daero, Iksan, Jeonbuk 54538, Republic of Korea.  
E-mail address: [jeanso@wku.ac.kr](mailto:jeanso@wku.ac.kr) (H.-S. So).

<sup>1</sup> These authors contributed equally to this work.

<https://doi.org/10.1016/j.yjmcc.2018.10.001>

Received 3 April 2018; Received in revised form 18 September 2018; Accepted 2 October 2018

Available online 03 October 2018

0022-2828/ © 2018 The Authors. Published by Elsevier Ltd. This is an open access article under the CC BY-NC-ND license

(<http://creativecommons.org/licenses/by-nc-nd/4.0/>).

induced by ROS generation, accompanied with depletion of antioxidant substances and increased lipid peroxidation lead to a systemic inflammatory response through the recruitment and release of pro-inflammatory mediators. As coincidental activation of nuclear factor (NF)- $\kappa$ B p65 and p53 has been linked to both apoptosis and inflammatory responses [5,6], which could be a significant factor in ADR-mediated cardiac injury.

Both intracellular NAD<sup>+</sup> and NADH levels are the fundamental metabolic regulators of cellular homeostasis and energy metabolism [7]. Regulation of cellular NAD<sup>+</sup> levels may have therapeutic benefits through its effect on NAD<sup>+</sup>-dependent enzymes, including sirtuins (SIRT1), and poly (ADP-ribose) polymerases (PARPs) [8]. Particularly, PARPs are plentiful ADP-ribosyl transferases that utilize NAD<sup>+</sup> to produce abundance of poly (ADP-ribose), which makes the staffing of DNA repair factors [9]. In response to DNA damage, PARP-1 can be mainly triggered by various patho-physiological conditions, such as ROS generation and inflammatory responses. Interestingly, cellular NAD<sup>+</sup> levels diminish due to the hyperactivation of PARP-1, which ultimately leads to apoptosis [10]. SIRT homologs (SIRT1–7), NAD<sup>+</sup>-dependent protein deacetylases regulate a variety of cellular processes, ranging from metabolism and energy stress response to tumorigenesis and aging [11]. Especially, nuclear SIRT1 is activated via energy stress conditions, namely exercise, fasting, or low glucose availability, and acts a vital role in metabolism, neurogenesis, hormone-stress response, and cell death [7] through deacetylation of substrates, i.e. p53, NF- $\kappa$ B and histones [12].

NAD(P)H quinone oxidoreductase 1 (NQO1) is an antioxidant flavoprotein enzyme that catalyzes the reduction and detoxification of quinones to hydroquinones by utilizing both NADH and NADPH as an electron donors, which thus increases cellular NAD<sup>+</sup> levels [13]. The elevated NAD<sup>+</sup>/NADH ratio induced by NQO1-mediated NADH oxidation can ameliorate the chief indications of metabolic symptoms [14]. Numerous NQO1 substrates have been recognized, including mitomycin C, RH1, AZQ, coenzyme Q10, idebenone, and  $\beta$ -lapachone [15,16]. Dunnione, an orange-red pigment extracted from *Streptocarpus dunnii* Mast, is usually recognized as an anti-fungal and anti-tumor agent, but has lately been shown to act as a powerful substrate of NQO1, leading to an increase in the intracellular NAD<sup>+</sup>/NADH ratio by NQO1 action, resulting in SIRT1 activation by using increased NAD<sup>+</sup> as a co-substrate [17]. Although the association between NAD<sup>+</sup>-dependent molecular and cellular events and various diseases is evident, it is unclear whether modulation of NAD<sup>+</sup> levels affects ADR-induced cardiomyopathy (AIC). In this study, we investigated the protective effects of dunnione on AIC in WT and NQO1<sup>-/-</sup> mice. Therefore, we found that dunnione protects against ADR-induced cardiac dysfunction and this effect is mediated by SIRT1 through NQO1 enzymatic action.

## 2. Methods

### 2.1. Drugs and chemicals

ADR was provided by Sigma-Aldrich Co. (St. Louis, MO, USA), and was dissolved in 0.9% sterile saline to achieve a final concentration of 2.0 mg/mL. Dunnione was chemically synthesized by Erum Biotechnologies, Inc. (Suwon, Korea) and micronized as particles. Antibodies against  $\gamma$ H2AX, H2AX, acetyl-NF- $\kappa$ B-p65, acetyl-p53, NF- $\kappa$ B-p65, p53, and SIRT1 were purchased from Cell Signaling Technology, Inc. (Beverly, MA, USA) and the internal control,  $\beta$ -actin was obtained from Santa Cruz Biotechnology, Inc. (CA, USA).

### 2.2. Mice

8–10 weeks-old-aged C57BL/6 male wild-type (WT) mice were obtained from the Central Laboratory Animal, Inc. (Seoul, Korea). On a C57BL/6 background, NQO1 knockout (NQO1<sup>-/-</sup>) mice were kindly provided by C.H. Lee (Animal Model Center, Korea Research Institute of

Bioscience and Biotechnology, Daejeon, Korea). All experiments were performed with same-aged healthy mice weighing between 22 and 24 g, and mice were age-matched within 5 days. All mice were fed a normal commercial diet and allowed free access to water during the experiment period, while kept at an ambient temperature of 20  $\pm$  2  $^{\circ}$ C and a relative humidity of 50  $\pm$  5% under a 12/12 h light/dark cycle in a specific pathogen-free facility. Mice studies were approved by the Animal Care and Use Committee of the Wonkwang University, Republic of Korea conducted in keeping with the standard guidelines.

### 2.3. Experimental designs

The experimental mice were arbitrarily categorized into four groups; group I: control group ( $n = 5$ ) received only normal saline, group II: ADR group ( $n = 5$ ) received three times intraperitoneal ADR injections (cumulative dose of 12 mg/kg i.p.; 4 mg/kg every day for 3 consecutive days), group III: ADR plus dunnione group ( $n = 5$ ) received intraperitoneal ADR injections and orally dunnione (20 mg/kg) administration, and group IV: dunnione alone group ( $n = 5$ ) received only dunnione orally administration over a period. ADR was intraperitoneally administrated on days 4 through 6 after 1 h exposure of dunnione. Body weight was measured every other day and also weighed on the day of sacrifice. After the last ADR injection on the fourth day, all mice were sacrificed by cervical dislocation. The heart tissues were immediately isolated, washed with phosphate buffered saline (PBS), and weighed. The heart tissue was excised; a portion of the left ventricle (LV) was rapidly frozen in liquid nitrogen, and then stored at  $-80^{\circ}$ C until further analyses.

### 2.4. Echocardiography

At the end of the treatment period, cardiac function in mice was analyzed by transthoracic echocardiography on day 4 after the last dose of ADR administration using a digital ultrasound system (Vivid S5 cardiovascular ultrasound system, GE healthcare, Yorba Linda, CA, USA) with a 30-MHz high frequency transducer. Briefly, the M-mode and two-dimensional echocardiography studies were evaluated along the short axis of the LV at the level of the papillary muscles after anesthetization in mice by inhalation of 1.5% isoflurane. The parameters of echocardiograms such as LV internal dimension-diastolic (LVIDd), LV internal dimension-systolic (LVIDs) and fractional shortening in percentage (FS%) were then assessed. All measurements were carried out at least three consecutive beats.

### 2.5. Histopathological analysis

For microscopy evaluation, heart tissues from mice were fixed in 4% formaldehyde and embedded in paraffin blocks. Paraffin embedded Sections (5- $\mu$ m thick) were deparaffinized in xylene, and rehydrated through ethanol-graded concentrations. Sections were stained with Hematoxylin and Eosin (HE) staining to observe the morphological changes of gross myocardial injury under a light microscope (IX71; Olympus, Japan) with DP analyzer software, using standard protocols. The histological cardiac injury scores of HE-stained heart sections were analyzed under a light microscope and scored based on the grade of myocardial degeneration (Supplemental Table S1). The samples were evaluated in a blinded manner by a single observer and ranked on a scale from 0 to 5; results are expressed as means  $\pm$  standard deviation (SD) of 10 representative fields/group. The morphological criteria for cardiac necrosis displaying myofibrillar loss and cytoplasmic vacuolization were defined in the method described previously [18].

TUNEL assay was used for the visualization of apoptotic cardiac cells using TUNEL TMR apoptosis detection kit; (Roche, Mannheim, Germany) according to the manufacture's instruction. Briefly, sections (5- $\mu$ m) were deparaffinized, rehydrated and then incubated with proteinase K (20 mg/mL). After blocking with endogenous peroxidase,

sections were incubated with 2% H<sub>2</sub>O<sub>2</sub> in methanol for 30 min at room temperature and washed in PBS, and then again incubated at 37 °C with labeling solution for 1 h. Nuclei were counterstained with DAPI (0.5 µg/mL; Molecular Probes, Eugene, OR, USA) at room temperature and finally examined under a fluorescence microscope (1 × 71; Olympus, Tokyo, Japan).

## 2.6. Measurement of plasma enzyme, oxidative marker, and pro-inflammatory cytokine levels

The blood was collected for determination of routine cardiac enzyme markers. The plasma levels of creatine phosphokinase (CPK), creatine kinase myocardial bound (CKMB), lactate dehydrogenase (LDH), and cardiac troponin I (cTnI) were estimated by using the commercial assay kits according to manufacturer's instructions (BioVision, USA). Oxidative damage in the cardiac tissues following various treatments was estimated by monitoring the levels of intracellular ROS, superoxide dismutase (SOD), reduced glutathione (GSH), and lipid peroxidation; malondialdehyde (MDA) in 10% tissue homogenates in PBS. The total intracellular ROS production was assessed according to the procedure described by Kim et al. [12]. In briefly, the fresh portions of heart tissues (100 µL) were incubated at 37 °C with 20 µM H<sub>2</sub>-DCFDA (2', 7'-dichlorodihydrofluorescein diacetate; Invitrogen, San Diego, CA, USA) for 1 h. Quantification of ROS level in the cardiac tissue was determined by DCF-F assay under a fluorescence spectrophotometer (excitation at 485 nm and emission at 525 nm). The fluorescence intensity was recorded under a CytoFluo series 4000 fluorometer and normalized in fold change with the control value. Determination of cardiac activities of reduced GSH, catalase, and SOD, and quantification of lipid peroxidation (MDA) were done by using their specific colorimetric assay kits (BioVision, USA) according to the manufacturer's instructions. Furthermore, the plasma protein levels of major pro-inflammatory cytokines, namely tumor necrosis factor- $\alpha$  (TNF- $\alpha$ ), interleukin (IL)-1 $\beta$ , and IL-6 were quantified using the commercially available mouse ELISA analysis kit (Quantikine Kit; R&D Systems, Minneapolis, MN, USA) according to the manufacturer's instructions.

## 2.7. Determination of NQO1 enzymatic activity and NAD(P)<sup>+</sup> / NAD(P)H ratio

The assay was measured using heart cytosolic fractions as described previously [19]. Concisely, NQO1 activity was analyzed by measuring the conversion rate of NADH to NAD<sup>+</sup> using 2,6-dichlorophenolindophenol (DCPIP) (Sigma). The decrease of NADH levels was calculated at 600 nm over 2 min. NQO1 activity was determined in a 1 mL reaction volume mixture containing cardiac cytosolic fractions, 200 µM NADH (Sigma-Aldrich), 40 µM DCPIP, Tris-HCl buffer (25 mM Tris-HCl, pH 7.4), and 0.7 mg/mL bovine serum albumin. Moreover, dicumarol (Sigma) was used to block NQO1 enzymatic reaction. The NAD(P)H/NAD(P)<sup>+</sup> ratio was determined using a commercial NADP<sup>+</sup> / NADPH assay kit (ECNP-100; BioAssay Systems, CA, USA) or NAD<sup>+</sup> / NADH assay kit (E2ND-100; BioAssay Systems). Briefly, the tissues were homogenized in either acidic extraction buffer for extraction of NAD(P)<sup>+</sup> or alkaline extraction buffer for extraction of NAD(P)H. Homogenates were heated at 60 °C for 5 min and then neutralized by addition of the opposite extraction buffer. An initial reading at 565 nm of a working reagent mix containing glucose-6-phosphate dehydrogenase (for NAD<sup>+</sup> / NADH) or lactate dehydrogenase plus diaphorase (for NADPH / NADP<sup>+</sup>) was taken immediately. Another reading was taken after a 15-min incubation period at room temperature. Calculation of total pyridine nucleotides was performed using an NAD(P)<sup>+</sup> standard curve.

## 2.8. Determination of SIRT1 activity

SIRT1 activity was measured using a fluorescent SIRT1 detection kit (Enzo Life Sciences International, Inc., PA, USA) following the manufacturer's protocol. In briefly, the SIRT1 activity was assayed using heart homogenates (40 µg/well), Fluor de Lys-SIRT1, NAD<sup>+</sup>, and SIRT1 assay buffer [25 mM Tris-HCl (pH 8.0), 137 mM NaCl, 2.7 mM KCl, 1 mM MgCl<sub>2</sub>, and 1 mg/mL BSA] in a 96-well plate. All reactions were originated by adding each substrate solution. After incubation at 37 °C for 1 h, the plate was further incubated with developing solution for 5 min. The deacetylated as a substrate was calculated by using the CytoFluo series 4000 fluorometer (PerSeptive Biosystems, Inc., Framingham, MA, USA) with the excitation (360 nm) and emission (460 nm) wavelengths.

## 2.9. Determination of PARP activity

PARP activity assay was determined using the Universal Chemiluminescent PARP assay kit (Trevigen, Gaithersburg, MD, USA) according to the manufacturer's protocols. The total tissue lysates (30 µg/well) were added into the wells containing PARP buffer cocktail, and then incubated at room temperature for 1 h. All wells were washed thrice with PBS plus 0.1% Triton X-100 (PBST), followed via incubation with a streptavidin-horseradish peroxidase in strep diluent buffer (1:1000 dilution) for 1 h. After extensively washes with PBST, chemiluminescent detection was performed. The background readings were subtracted from the readings of samples, and PARP activity was analyzed using a standard curve.

## 2.10. Western blotting

For protein analysis, heart tissues were homogenized with cold lysis buffer and lysates were calculated using the Bio-Rad protein assay kit (Bio-Rad Laboratories, Hercules, CA, USA). Equal amount of protein lysates (40 µg) were subjected to electrophoresis on 10% sodium dodecyl sulfate-polyacrylamide gels (SDS-PAGE) for 3 h at 20 mA, and then transferred to nitrocellulose membranes. The membranes were blocked with 5% dried milk protein in tris buffered saline PBS containing 0.04% Tween 20 (TBST) for 1 h, washed 3 times with TBST every 10 min. The membranes treated with primary antibodies (1:1000) were incubated at 4 °C overnight. After extensively washing with TBST, membranes were again incubated at room temperature with appropriate secondary antibodies for 1 h and washed with TBST 3 times. The protein bands on membranes were developed using enhanced chemiluminescent reagents (Supersignal Substrate; Pierce, Rockford, IL, USA) following the manufacturer's instructions. The densities of detected protein bands were quantified with densitometric analysis by Scion Image program (Epson GT-X700; Tokyo, Japan). All values were normalized by setting the density of control samples as 1.0.

## 2.11. Quantitative real-time PCR (qRT-PCR) for miR-34a and pro-inflammatory cytokines

For determination of miR-34a expression, the RNA fractions was extracted from isolated cardiac cells using a mirVana miRNA isolation kit (Ambion, Austin, TX, USA) according to the manufacturer's instructions. This extracted total RNA was reverse transcribed by using Taqman miRNA Reverse Transcription Kit, and then amplified in a 20 mL PCR with primer set for amplification of miR-34a (Assay ID: 000426) and U6 (Assay ID: 001093) by using TaqMan<sup>®</sup> miR assays according the kit's protocol. The amplification step pursued by 40 cycles of denaturation at 95 °C for 15 s and then annealing at 60 °C for 1 min, were carried out on the LightCycler PCR system (Roche Applied Science) using the TaqMan Universal PCR master Mix. All relative levels were evaluated using the  $\Delta\Delta C_t$  (threshold cycle value) method with U6 as an endogenous control. For evaluation of pro-inflammatory cytokines, RNA was isolated from heart tissues (20 mg) using TRIzol

(Invitrogen, CA, USA) following the manufacturer's instruction. Total RNA (2–3 µg) was translated to cDNA using First strand cDNA synthesis Superscript kit (Invitrogen) according to the manufacturer's protocol. The resulting cDNA was performed to RT-PCR (LightCycler® Nano software) using SYBR Green Mastermix (Invitrogen). The qRT-PCR used primers were as follows: TNF- $\alpha$ , 5'-CTGAGGTCAATCTGCCCAAGTAC-3' and 5'-CTTCACAGAGCAATGACTCCAA AG-3'; IL-1 $\beta$ , 5'-TCTTTGAAGTTGACGGACCC-3' and 5'-TGAGTGATACTGCCTGCCTG-3'; IL-6, 5'-TCGTGGAATGAGAAAAGAGTTG-3' and 5'-AGTGCATCATCGTTGTTTCATACA-3'; COX-2, 5'-GGGTTAACTTCCAAAGGAGACATC-3' and 5'-CAGCCTGGCAAGTCTTTAA CCT-3'; MCP1, 5'-GCT GGAGAGCTACAAGAGATCA-3' and 5'-ACAGACCTCTCTTG AGCTTGGT-3'; iNOS, 5'-GGGCTGTACGGAGATCA-3' and 5'-CCATGATGGTCACATT CTGC-3'; GAPDH, 5'-TCCACTCTTCCACCTTCGA-3' and 5'-AGTTGGGATAGGGCCTCT CTTG-3'. GAPDH was used for normalization, and all relative mRNA expressions were quantified by  $\Delta\Delta C_t$  method. All results were carried out expressed as change in fold relative to control.

### 2.12. Assessment of NOX activity

NOX activity was quantified based on the reduction of cytochrome *c* in heart tissues. Reduction of cytochrome *c* was determined by reading the absorbance changes at 550 nm for 3 min in the presence or absence of the NOX inhibitor diphenylethiodonium (DPI; 100 µM). DPI-inhibitable activity [(absorbance changes in the absence of DPI) – (absorbance changes in the presence of DPI)] was taken as NOX activity. The results were expressed as fold change.

### 2.13. Statistical analysis

Statistical differences of all results were determined by one-way analysis of variance (ANOVA), and *p* values were reported. Each experiment was performed at least thrice, and all results stand for mean  $\pm$  standard error of the mean (SEM) of triplicate analyses. All statistical data were calculated using OriginPro 6.1 software by a master level biostatistician, and considered statistically significant when *p* values were < 0.05.

## 3. Results

### 3.1. Dunnione has a cardioprotective effect on mice treated with ADR, and attenuates ADR-induced cardiac dysfunction

To determine the effect of dunnione on ADR-induced cardiomyopathy (AIC), we treated C57BL/6J WT and NQO1<sup>-/-</sup> mice with dunnione, ADR, or ADR plus dunnione as described in Supplemental Fig. S1A. We first assessed the cardiac function by echocardiography in WT and NQO1<sup>-/-</sup> mice on day 4 after the last ADR exposure. As shown in Fig. 1A and Supplemental Fig. S1B, both LVIDd and LVIDs significantly increased in the ADR group of WT mice, but the cardiac contractility reflected by the FS in WT mice decreased. However, these changes were remarkably restored in WT mice treated with ADR plus dunnione. Since dunnione is a substrate for NQO1, we next conducted similar experiments using NQO1<sup>-/-</sup> mice to investigate whether the protective effect induced by dunnione is mediated by the NQO1 enzymatic action. In contrast, we found that changes in cardiac dysfunction in ADR-treated NQO1<sup>-/-</sup> mice were not improved by dunnione (Fig. 1B–Supplemental Fig. S1B). Moreover, the changes in mean body weight, heart weight, and heart-to-body weight ratio indicated signs of cardiac atrophy among the four groups of WT and NQO1<sup>-/-</sup> mice (Fig. 1C–F), and tended to decrease significantly by ADR administration. However, dunnione improved these deleterious changes by ADR in WT, but not in NQO1<sup>-/-</sup> mice (Fig. 1C–F). These results strongly suggest that the cardioprotective effect of dunnione on ADR-induced cardiomyopathy is mediated through NQO1.

### 3.2. Dunnione ameliorates ADR-induced acute myocardial injury

The pathophysiology of ADR-induced cardiac injury is defined as myocardial degeneration or tissue destruction in the manner of myofibrillar loss and cytoplasmic vacuolization [20]. To assess the protective effect of dunnione on ADR-induced cardiac damage, we examined the cardiac section by H/E staining in an experimental WT and NQO1<sup>-/-</sup> mice. As compared to control mice, ADR-treated WT mice histologically showed marked myocardial degeneration (i.e., myofibrillar loss or disorganization and cytoplasmic vacuolization) in the ventricles (Fig. 2A), which are characteristic features of myocardial cell damage [3]. These pathological harmful effects were largely abolished by dunnione in WT (Fig. 2A). We also quantified the cardiac injury score via the assessment criteria described in the Methods section (Supplemental Table S1). As expected, ADR significantly increased the severity of cardiac injury (2.65  $\pm$  0.42) compared to the control, but dunnione markedly alleviated the ADR-induced myocardial injury (0.69  $\pm$  0.2) (Fig. 2A). The characteristics of cardiologic histology in the dunnione alone group were similar to those of the control group. We also analyzed the biochemical markers involved in myocardial damage and histological features in ADR-treated NQO1<sup>-/-</sup> mice. Histologically, ADR treatment of NQO1<sup>-/-</sup> mice also resulted in typical cardiac damage similar as ADR-treated WT mice. Unlike the WT results, dunnione did not show protective effects on ADR-induced cardiac damage in NQO1<sup>-/-</sup> mice (Fig. 2B), including histological damage scores (ADR alone: 2.8  $\pm$  0.46; ADR plus dunnione: 2.9  $\pm$  0.52). In addition, the plasma concentrations of CPK, CKMB, cTnI, and LDH, the major clinical endpoints of cardiac dysfunction and injury, were measured at day 4 after the last ADR treatment. ADR significantly elevated the plasma levels of CPK, CKMB, cTnI, and LDH in ADR-treated WT mice as compared to control mice (Fig. 2C). However, ADR plus dunnione group showed significantly reduced plasma levels of all biochemical biomarkers (Fig. 2C). Conversely, the increased plasma levels of all major biomarkers in ADR-treated NQO1<sup>-/-</sup> mice showed no significant differences from those observed in ADR-treated WT mice. However, dunnione did not decrease the plasma levels of the biomarkers increased by ADR in NQO1<sup>-/-</sup> mice (Fig. 2D). To confirm the role of NQO1 action in ADR-induced myocardial injury, we treated C57BL/6J WT and NQO1<sup>-/-</sup> mice with  $\beta$ -lapachone (a well-known NQO1 substrate), ADR, or ADR plus  $\beta$ -lapachone. As shown in Supplemental Fig. S2, the changes in mean body weight and heart weight indicated signs of cardiac atrophy among the four groups of mice, and tended to decrease significantly by ADR administration. However,  $\beta$ -lapachone improved these deleterious changes by ADR in WT mice. In addition, ADR plus  $\beta$ -lapachone group showed significantly reduced plasma levels of CPK and cTnI in WT, but not in NQO1<sup>-/-</sup> mice (Supplemental Fig. S2). These results indicate that NQO1 activation using dunnione or  $\beta$ -Lap as substrates has protective effects against ADR-induced acute cardiac damage.

### 3.3. Dunnione treatment protects against ADR cardiotoxicity, which is mediated by cardiac cell apoptosis

A previous study indicated that increased cell death in cardiac tissues contributes to the pathogenesis of ADR-induced cardiomyopathy [21]. As Cardiac dysfunction and damage in WT mice was obviously induced by ADR, but not in the mice treated with ADR plus dunnione (Figs. 1–2), we next examined whether dunnione affected ADR-induced apoptotic death of cardiac myocytes using TUNEL assay. Therefore, we found that the number of TUNEL-positive nuclei in the ventricular myocardium of WT mice, which implies apoptotic death of cells, was increased by ADR exposure compared to normal control mice, but significantly decreased in whole heart area during dunnione treatment (Fig. 3A). Interestingly, unlike the WT results, increased numbers of TUNEL-positive nuclei by ADR in the cardiac tissue of NQO1<sup>-/-</sup> mice were not reduced by additional treatment with dunnione (Fig. 3B).

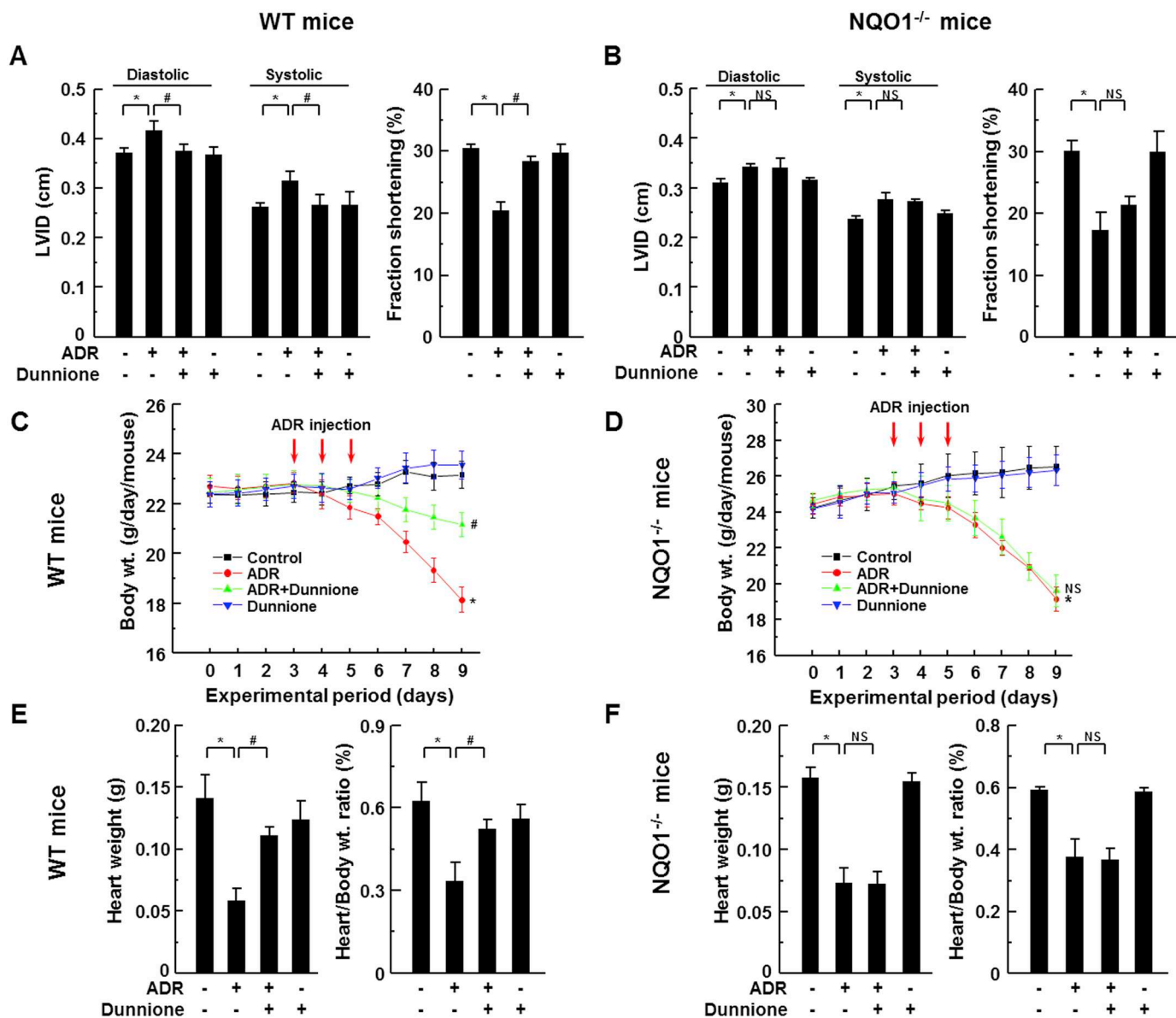


**Fig. 1.** Protective effect of dunnione on ADR-induced cardiac dysfunction. Dunnione (20 mg/kg body weight) was orally administered daily from the first day of the experiment. 1 h after administration of dunnione, ADR (12 mg/kg body weight) was injected once a day for three consecutive days. **A–B.** Two-dimensional M-mode echocardiograms and quantitative group data for echocardiographic measurements: LVIdD (cm), LVIDs (cm), and FS (%) were assessed by echocardiography on day 4 after the last dose of ADR injection in WT (**A**) and NQO1<sup>-/-</sup> (**B**) mice. **C–F.** The changes in daily body weight, heart weight, and heart weight/body weight ratio were measured in WT (**C–E**) and NQO1<sup>-/-</sup> (**D–F**) mice. Data in grams (g) are presented as mean  $\pm$  standard error of the mean (SEM). Red (\*) and green (#) indicate  $p < 0.05$ , by one-way ANOVA, suggesting statistically significant differences between baseline-corrected body weights of ADR- and saline-treated control mice at day 5 through day 11. NS, not significant; ( $n = 5$ ). LVIdD, left ventricular internal dimension-diastolic; LVIDs, left ventricular internal dimension-systolic; FS, fractional shortening. (For interpretation of the references to colour in this figure legend, the reader is referred to the web version of this article.)

Overall, this result strongly suggests that NQO1 is critically required for the protective effects of dunnione against ADR-induced cardiac degeneration and cardiotoxicity.

#### 3.4. Dunnione attenuates PARP-1 hyperactivation by ADR-induced DNA damage, and prevents reduced intracellular NAD<sup>+</sup>/NADH ratio

There are some evidences that ADR therapy induces higher ROS production in the heart, which can lead to ADR-induced cardiac toxicity through oxidative stress [22] and DNA damage [23]. Previous studies have shown that NADPH oxidase (NOX) is a major source of ROS in ADR-induced cardiac toxicity and is regulated by NADPH, a rate-limiting substrate for NOX activation. Therefore, we examined the effects of dunnione on the cellular ratio of NADPH/NADP<sup>+</sup>, NOX activity, and

oxidative stress related parameters including lipid peroxidation in cardiac tissues of ADR-treated mice. As expected, ADR-treated WT mice showed significantly increased intracellular NADPH/NADP<sup>+</sup> ratio, NOX activity and lipid peroxidation (MDA) compared to the control group, but showed significantly reduced catalase, and SOD activity (Fig. 4A). However, these deleterious effects were attenuated by dunnione (Fig. 4A). In contrast, the changes of NADPH/NADP<sup>+</sup> ratio, NOX activity and antioxidant enzymes in ADR-treated NQO1<sup>-/-</sup> mice were not improved by dunnione (Fig. 4B). Consistently, the phosphorylation of H2AX, which is indicative of DNA damage, was reduced by dunnione in the heart tissue of ADR-treated WT mice, but not in NQO1<sup>-/-</sup> mice (Fig. 4E–F).

As the excessive hyperactivation of PARP-1 shifts negatively charged ADP-ribose groups i.e. PARylation from NAD<sup>+</sup> to itself or

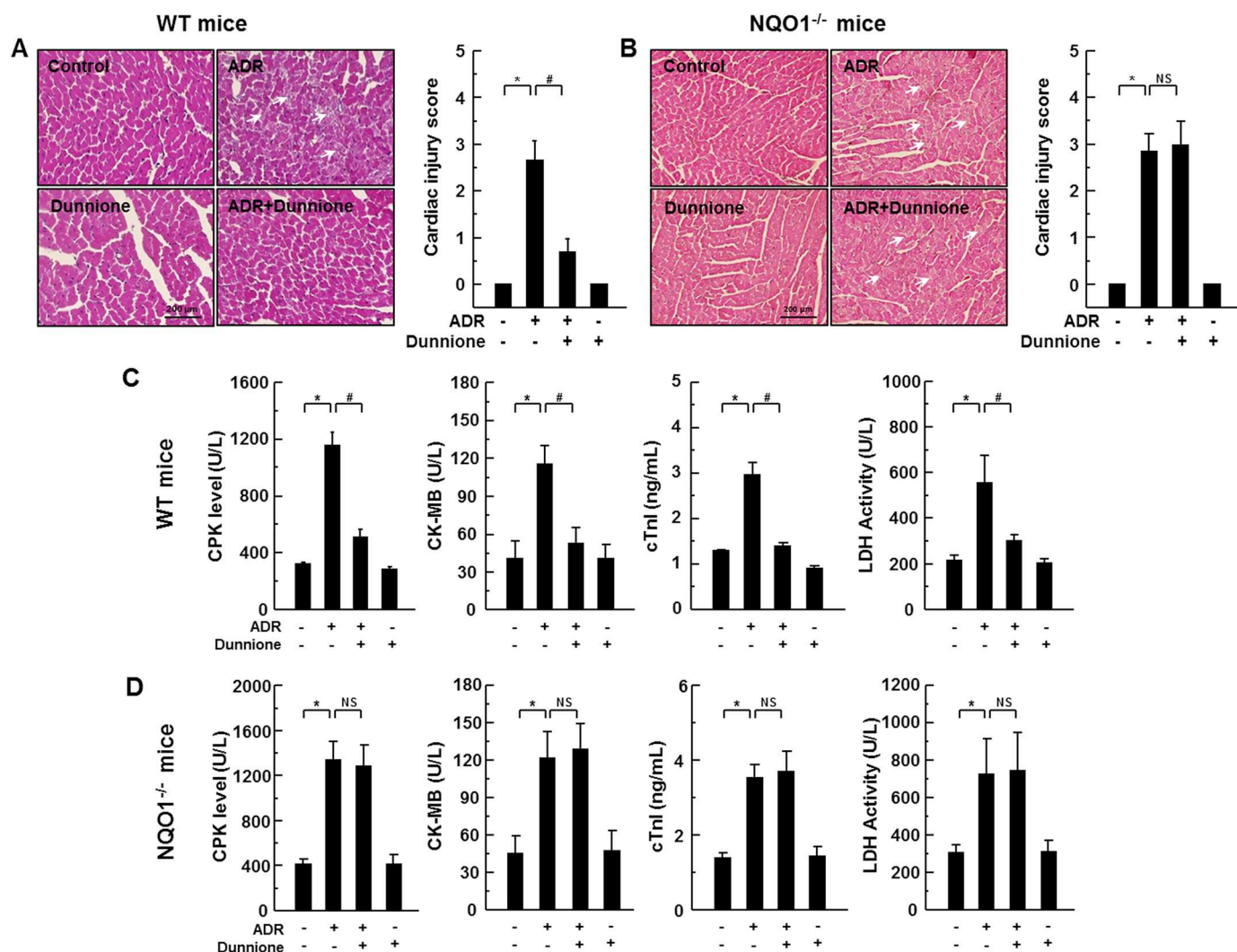


**Fig. 2.** Cardioprotective effect of dunnione on ADR-induced cardiac damage. Dunnione (20 mg/kg body weight) was orally administered daily from the first day of the experiment. 1 h after administration of dunnione, ADR (12 mg/kg body weight) was injected once a day for three consecutive days. **A–B.** Mice were sacrificed at 4 days after the last dose of ADR injection, the heart tissues were isolated and stained with hematoxylin and eosin Y stain, and examined under a light microscope in WT (**A**) and NQO1<sup>-/-</sup> (**B**) mice. Control, normal saline (0.9% NaCl)-treated group; ADR, 12 mg/kg ADR only group; ADR + dunnione, ADR and 20 mg/kg dunnione combined group; dunnione, 20 mg/kg dunnione only group. Damaged areas were indicated with black arrows, and 10 fields of 400 $\times$  of cardiac injury were scored using the quantitative evaluation method described in Supplemental Table 1. **C–D.** The plasma levels of CPK (U/L), CKMB (U/L), cTnI (ng/mL), and LDH (U/L) were analyzed in WT (**C**) and NQO1<sup>-/-</sup> (**D**) mice. Data are presented as mean  $\pm$  SEM. \* and # indicate  $p < 0.05$ , by one-way ANOVA compared with the control (\*) and ADR alone group (#). NS, not significant; ( $n = 5$ ; Scale bar: 200  $\mu$ m). CPK, creatine phosphokinase; CKMB, creatine kinase-MB; cTnI, cardiac Troponin I; LDH, lactate dehydrogenase.

target proteins in response to DNA damage, and then regulates transcription, DNA repair, and mitochondrial function. Therefore, PARylation of PARP-1 facilitates the staffing of DNA repair factors [24]. However, hyperactivation of PARP-1 can deplete intracellular NAD<sup>+</sup> and cause subsequent tissue damage [12]. We assessed the effect of dunnione on PARP activation in the heart tissue of ADR-treated WT mice (Fig. 5A). As compared to control, PARP activity was markedly increased after ADR treatment, and this increase was significantly inhibited by dunnione in WT mice (Fig. 5A), but not in NQO1<sup>-/-</sup> mice (Fig. 5B). Dunnione is a potent NQO1 substrate that oxidizes NADH to NAD<sup>+</sup>, thus increasing the cellular NAD<sup>+</sup>/NADH ratio [17,25]. Thus, we next examined the effect of dunnione on NQO1 activity and cellular NAD<sup>+</sup>/NADH ratio in the cardiac tissue of ADR-treated WT mice or NQO1<sup>-/-</sup> mice. As shown in Fig. 5C and D, the NQO1 activity and intracellular NAD<sup>+</sup>/NADH ratio of WT mice were significantly lower than those of control group after ADR exposure, and dunnione induced this cellular NAD<sup>+</sup>/NADH ratio close to the control level (Fig. 5C–D). On the other hand, the cellular NAD<sup>+</sup>/NADH ratio of the cardiac tissue

of NQO1<sup>-/-</sup> mice was significantly reduced by ADR similar to that of WT mice. However, unlike the WT results, dunnione did not reduce the decrease of cellular NAD<sup>+</sup>/NADH ratio after ADR exposure in NQO1<sup>-/-</sup> mice (Fig. 5E).

### 3.5. Dunnione reinstates ADR-induced SIRT1 activity and protein expression via the modulation of acetylated p53 and miR-34a expression

SIRT1, NAD<sup>+</sup>-dependent protein deacetylase, has been linked in ADR-induced cardiac toxicity [26]. Since SIRT1 also uses NAD<sup>+</sup> in cells during stress response, PARP-1 activation has a significant effect on SIRT1 function. Accumulating studies prove that miR-34a is a negative regulator of SIRT1 as well as downstream effector of p53 [27]. It has also been reported that p53-mediated miR-34a induction downregulates SIRT1 protein expression and activity in an acute pancreatitis model, but increase in cellular NAD<sup>+</sup> by NQO1 enzymatic action suppresses acute pancreatitis through modulation of the p53-mediated miR-34a pathway [28]. Therefore, we examined whether dunnione

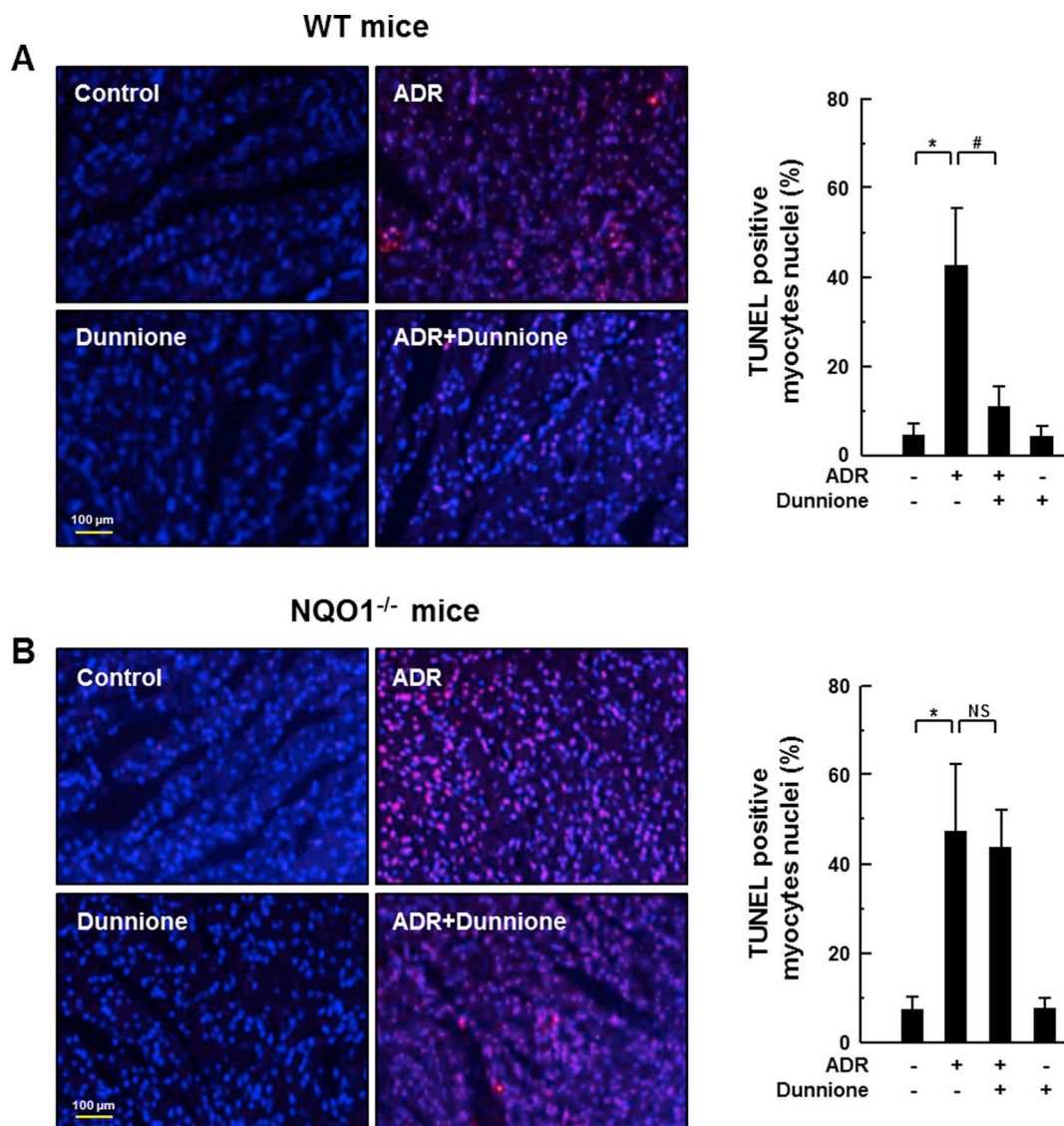


**Fig. 3.** Effect of dunnione on ADR-induced apoptotic cell death in the heart tissues of C57BL/6 mice. Dunnione (20 mg/kg body weight) was orally administered daily from the first day of experiment. 1 h after administration of dunnione, ADR (12 mg/kg body weight) was injected once a day for three consecutive days. **A–B.** TUNEL-positive nuclei were identified by TUNEL staining and examined under a fluorescent microscope in WT (**A**) and NQO1<sup>-/-</sup> (**B**) mice. Apoptotic cells were visualized as pink. Counterstaining for the nuclei was conducted with DAPI and visualized as blue. Control, normal saline (0.9% NaCl)-treated group; ADR, 12 mg/kg ADR only group; ADR + dunnione, ADR and 20 mg/kg dunnione combined group; dunnione, 20 mg/kg dunnione only group. Quantitative analysis of TUNEL-positive nuclei in percentage (%). \* and # indicate  $p < 0.05$  by one-way ANOVA compared with the control (\*) and ADR alone group (#), NS, not significant; ( $n = 5$ ; Scale bar: 100  $\mu\text{m}$ ). (For interpretation of the references to colour in this figure legend, the reader is referred to the web version of this article.) (For interpretation of the references to colour in this figure legend, the reader is referred to the web version of this article.)

affects SIRT1 expression and activity in the cardiac tissues of ADR-treated WT or NQO1<sup>-/-</sup> mice. Although SIRT1 mRNA levels were not affected by ADR or dunnione (data not shown), the protein expression and activity of SIRT1 in the cardiac tissue of WT mice were significantly reduced after ADR exposure, but were clearly prevented by dunnione (Fig. 6A and C). However, ADR-induced decrease in SIRT1 protein expression and activity in the cardiac tissue of NQO1<sup>-/-</sup> mice was not significantly prevented by dunnione (Fig. 6B–D). To confirm that SIRT1 was critically required for the protective effects of dunnione, we investigated cell viability in H9c2 cardiomyocytes after exposure of ADR or dunnione in the presence of nicotinamide (SIRT1 inhibitor). As shown in Supplemental Fig. S5, dunnione significantly ameliorated ADR-induced cytotoxicity, as evidenced by an increase in cell viability. However, pretreatment of the H9c2 cells with nicotinamide (NAM) prior to the exposure to dunnione plus ADR abolished the protective effect of dunnione, resulting in a significant decrease in cell viability.

These results suggest that SIRT1 is critically required for the protective effects of dunnione against ADR-induced cardiotoxicity. In addition, miR-34a expression was significantly elevated in the cardiac tissue following ADR exposure, which was completely inhibited by dunnione in WT mice but not in NQO1<sup>-/-</sup> mice (Fig. 6E–F). As previously demonstrated, ADR induces the activation of acetylated p53 [29], a key mediator and upstream regulator of miR-34a [28]. Therefore, we assessed whether dunnione reduced ADR-induced acetylation of p53 in the cardiac tissue. As compared to control, western blot analysis indicated that ADR treatment of WT mice significantly increased p53 acetylation without change in total p53 protein level, whereas dunnione completely suppressed acetylation of p53 (Fig. 6G). However, this effect of dunnione was completely attenuated in NQO1<sup>-/-</sup> mice (Fig. 6H).

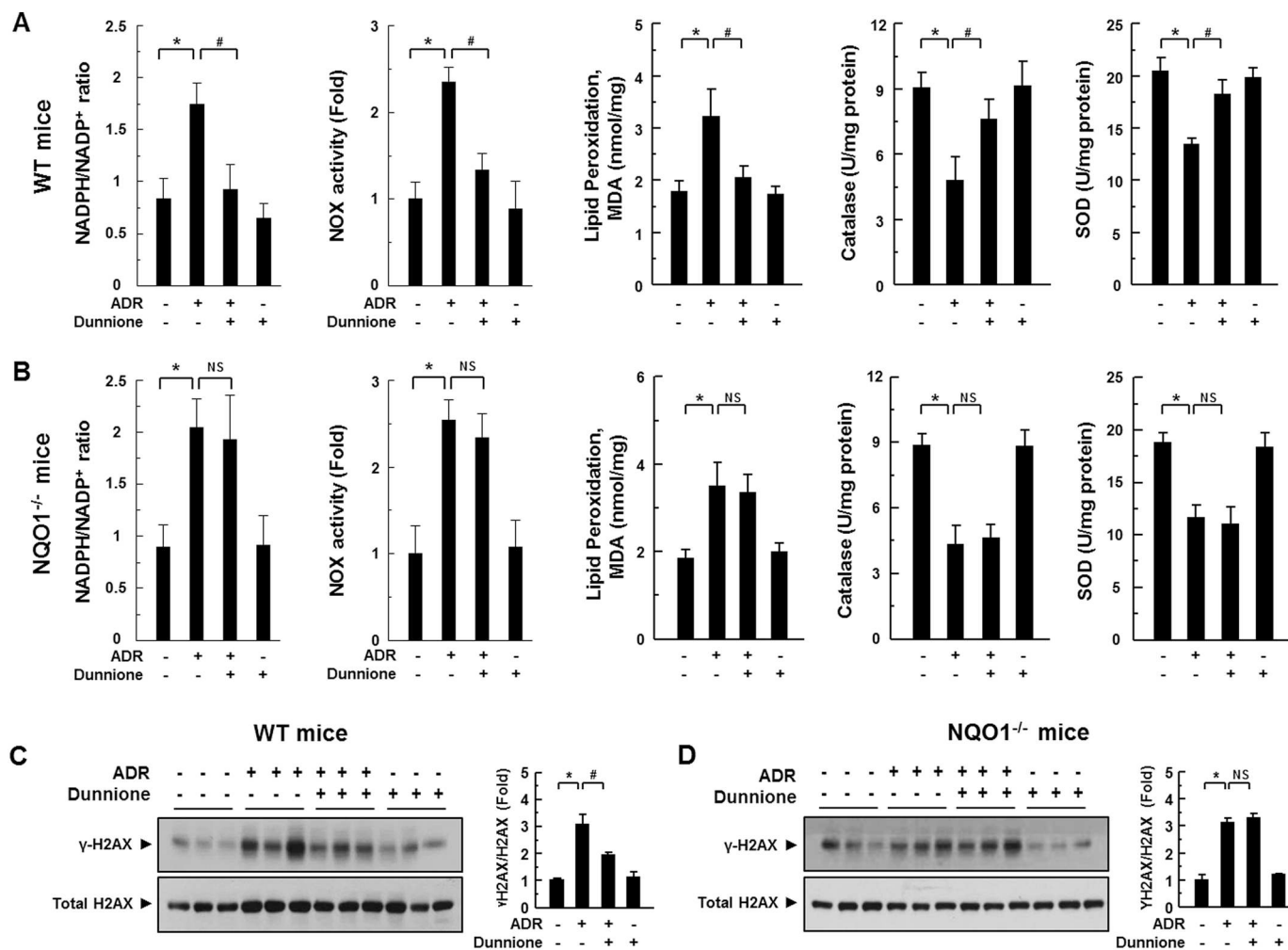


**Fig. 4.** Effect of dunnione on ADR-induced ROS generation and other major oxidative markers, and DNA damage. Dunnione (20 mg/kg body weight) was orally administered daily from the first day of the experiment. 1 h after administration of dunnione, ADR (12 mg/kg body weight) was injected once a day for three consecutive days. The heart tissue was isolated at day 4 after the last dose of ADR injection, and then NADPH/NADP<sup>+</sup> ratio, NOX activity, MDA (nmol/mg), Catalase (U/mg protein), and SOD (U/mg protein) were assessed by colorimetric assay kits in WT (A) and NQO1<sup>-/-</sup> (B) mice. C–D. DNA damage was analyzed by western blotting using anti-γH2AX antibody in WT (C) and NQO1<sup>-/-</sup> (D) mice. \* and # indicate  $p < 0.05$  by one-way ANOVA compared with the control (\*) and ADR alone group (#), NS: not significant; (n = 5). MDA, malondialdehyde; SOD, superoxide dismutase.

### 3.6. Dunnione inhibits acetylation of NF-κB p65 and production of pro-inflammatory mediators induced by ADR

Previous studies have demonstrated that NF-κB plays a crucial role in regulating genes that contribute to the onset of ADR-induced oxidative stress, pro-inflammatory responses, and apoptosis in cardiac tissues [30,31]. Furthermore, NF-κB regulates the expression of various pro-inflammatory cytokines and chemokines that are involved in ADR-induced cardiac toxicity [32]. In addition, NF-κB activity is regulated via post-translational modifications, namely phosphorylation and acetylation. Current studies have suggested that the incapability of reduced SIRT1 activity to deacetylate the NF-κB subunit p65 at lysine-310 aggravates the inflammatory mediators [12,17,28]. Interestingly, the level of acetylated NF-κB p65 was strongly increased in the cardiac tissue of ADR-treated WT mice compared with control, and this effect was significantly suppressed by dunnione (Fig. 7A). In contrast, inhibition of ADR-induced NF-κB p65 acetylation by dunnione was not observed in NQO1<sup>-/-</sup> mice (Fig. 7B). The mRNA and protein expression levels of pro-inflammatory cytokines (TNF-α, IL-1β, and IL-6) were increased in the cardiac tissue of ADR-injected WT mice. However, their levels were significantly attenuated in WT mice by dunnione treatment (Fig. 7C-Supplemental Fig. S2A). Unlike the effect of dunnione in WT

mice, the increase in mRNA and protein levels of pro-inflammatory cytokines after ADR exposure was not attenuated by dunnione in NQO1<sup>-/-</sup> mice (Fig. 7D-Supplemental Fig. S2B). Similar to pro-inflammatory cytokine mRNA expression patterns, increased mRNA levels of COX-2, iNOS, and MCP-1 induced by ADR were significantly reduced by dunnione in the cardiac tissues of WT mice, but not in NQO1<sup>-/-</sup> mice (Fig. 7E–F), suggesting that dunnione ameliorates cardiac inflammation by downregulating NF-κB signaling. Taken together, these results strongly suggested that the induction of the cellular NAD<sup>+</sup> levels using dunnione attenuated ADR-induced cardiomyopathy via the regulation of PARP-1 and SIRT1 activity.

## 4. Discussion

Despite the beneficial effects of ADR as a potent chemotherapeutic agent, the onset of cardiomyopathy leading to heart failure remains an important issue in oncology and cardiology [33,34]. Although the underlying molecular mechanism has not been fully elucidated, an alternative approach to reduce its cardiotoxicity has important clinical relevance [35]. ADR cardiotoxicity is associated with oxidative stress mainly by ROS production and is a complex multiple factor process with increased antioxidant depletion and increased lipid peroxidation,

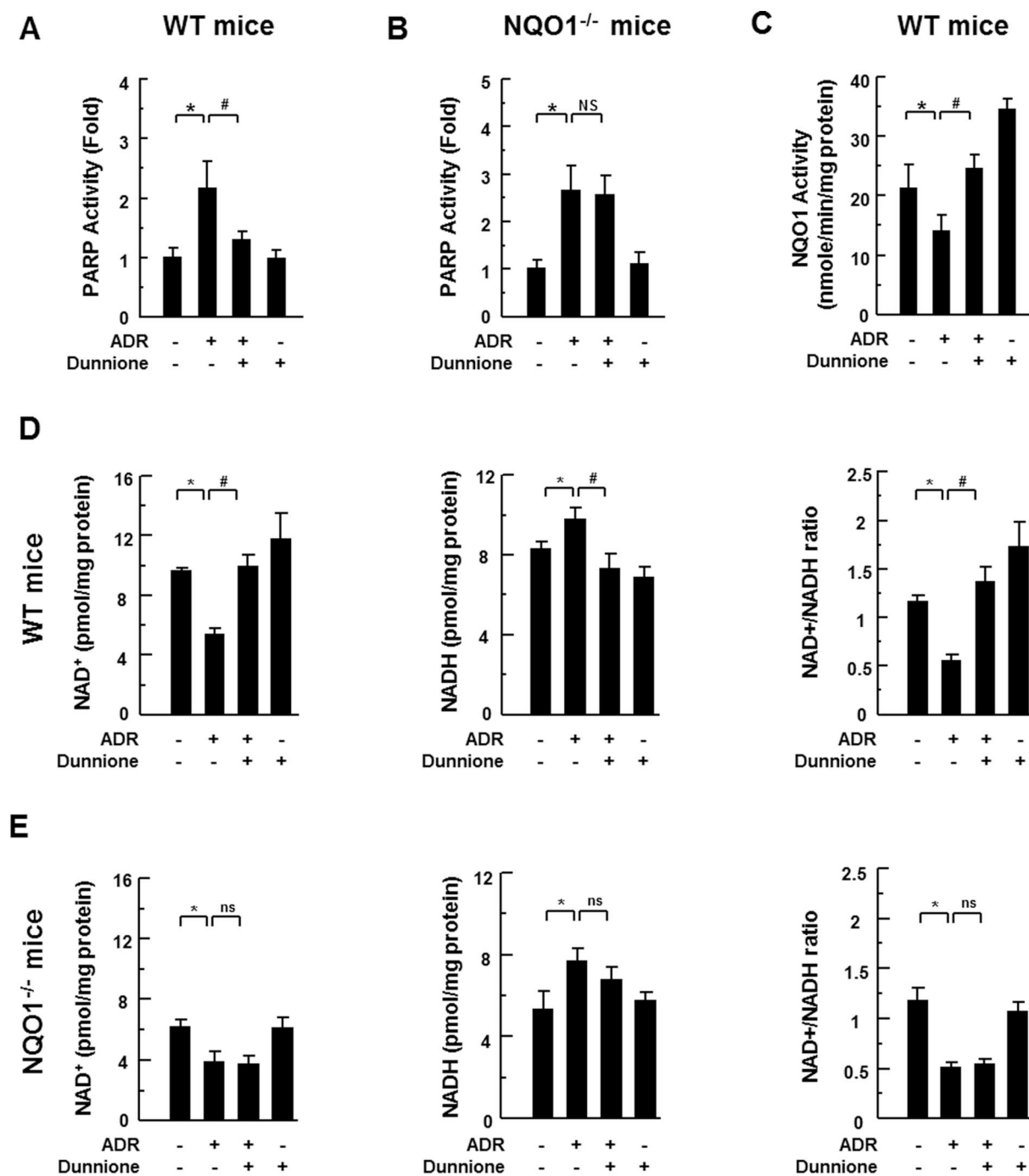


**Fig. 5.** Effect of dunnione on PARP-1 activation, NQO1 activity, and cellular NAD<sup>+</sup>/NADH ratio in ADR-treated mice. Dunnione (20 mg/kg body weight) was orally administered daily from the first day of the experiment. 1 h after administration of dunnione, ADR (12 mg/kg body weight) was injected once a day for three consecutive days. A–E. The heart tissue was isolated at day 4 after the last dose of ADR injection. PARP activity, NQO1 activity and NAD<sup>+</sup>/NADH ratio were assayed using the PARP, NQO1, and NAD<sup>+</sup>/NADH assay kits, respectively, in WT (A, C, D) and NQO1<sup>-/-</sup> (B, E) mice. \* and # indicate  $p < 0.05$  by one-way ANOVA compared with the control (\*) and ADR alone group (#). NS, not significant; (n = 5).

leading to systemic inflammatory responses through the recruitment and release of pro-inflammatory mediators. NF- $\kappa$ B p65 and p53 may be important factors in ADR-mediated cardiac damage, since co-incidental activation of these molecules is associated with inflammatory responses and apoptosis [5,6]. It is generally believed that ROS generation plays a critical role in ADR-induced p53 activation through oxidative DNA damage [36]. Therefore, NF- $\kappa$ B and p53 have been illustrated as key mediators of ADR-induced toxicity because of their contribution in DNA damage, oxidative stress and inflammation via a mutual feedback procedure of ‘cause and effect’. Of note, it has been reported that

activation of p53 and NF- $\kappa$ B p65 is associated with ADR-induced cardiomyocyte apoptosis [37,38]. Furthermore, the activation of acetylated p53 was also critically involved in ADR-induced cardiac damage [39]. In our study, we determined the effect of NAD<sup>+</sup> metabolism on ADR-induced cardiac dysfunction. Our results suggest that the reduction in SIRT1 activity and protein expression may be associated with decreased intracellular NAD<sup>+</sup> levels, and play an important role in advance of ADR-induced cardiac dysfunction. Reduced SIRT1 activity attenuated deacetylation of downstream targets namely p53 and NF- $\kappa$ B, which are highly activated by acetylation, and exacerbated ADR-

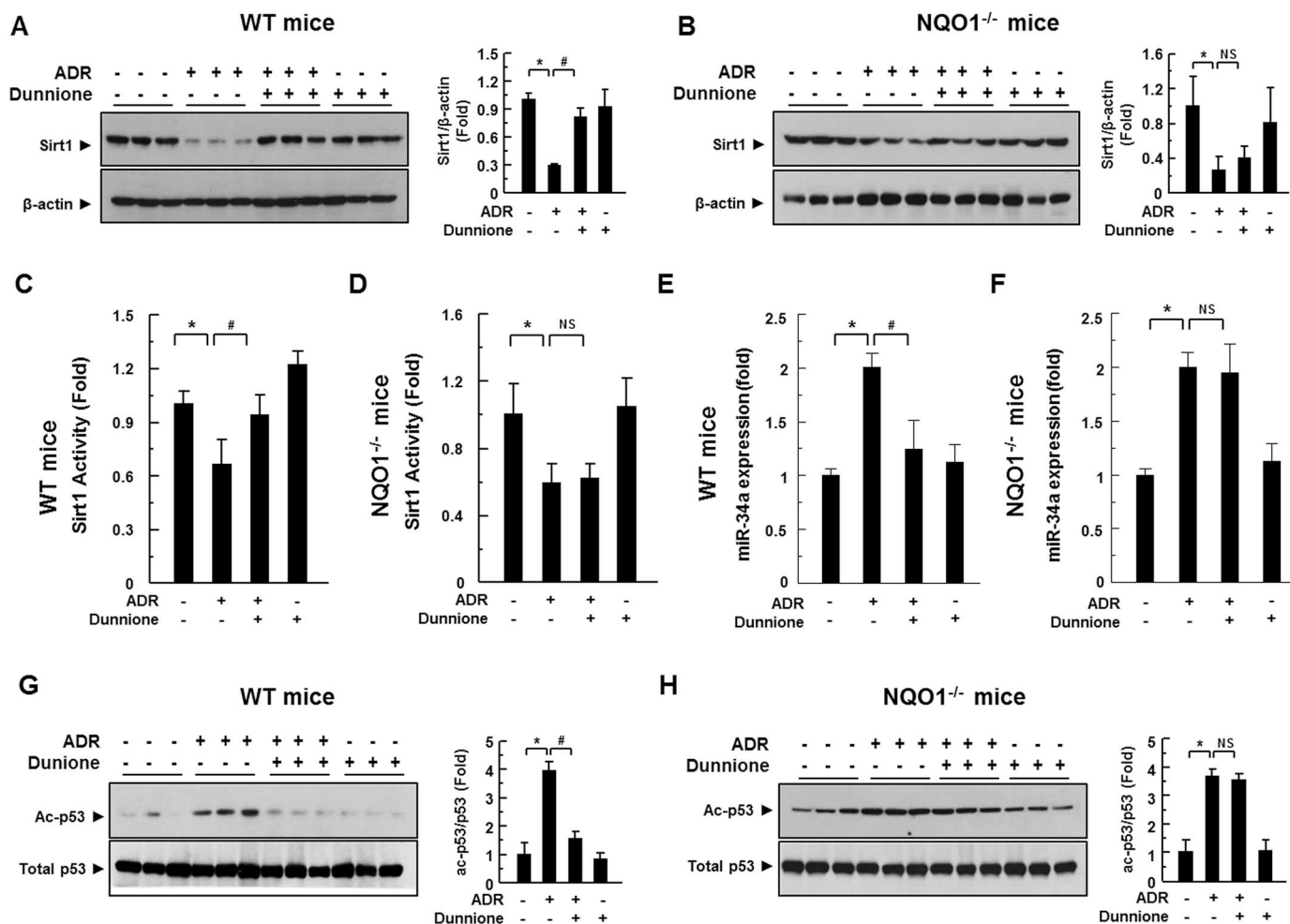


**Fig. 6.** Effect of dunnione on SIRT1 expression and its activity. Dunnione (20 mg/kg body weight) was orally administered daily from the first day of the experiment. 1 h after administration of dunnione, ADR (12 mg/kg body weight) was injected once a day for three consecutive days. A–B. The heart tissue was isolated at day 4 after the last dose of ADR injection. The level of SIRT1 protein was analyzed by western blotting in WT (A) and NQO1<sup>-/-</sup> (B) mice. Densitometric analysis is presented as the fold induction of SIRT1 relative to β-actin. C–D. SIRT1 activity was measured using SIRT1 assay kit in WT (C) and NQO1<sup>-/-</sup> (D) mice. E–F. Levels of miR-34a expression were analyzed by quantitative RT-PCR in WT (E) and NQO1<sup>-/-</sup> (F) mice. G–H. Acetylated p53 and total p53 levels were determined by western blotting using anti-acetylated p53 and anti-p53 antibodies in WT (G) and NQO1<sup>-/-</sup> (H) mice. \* and # indicate  $p < 0.05$  by one-way ANOVA compared with the control (\*) and ADR alone group (#). NS, not significant; (n = 5).

induced cardiac dysfunction through inflammation responses and apoptosis. However, dunnione prophylactically attenuated ADR-induced cardiac dysfunction in an NQO1-dependent manner and decreased cardiac tissue damage by reducing ROS production and PARP activation. Dunnione also reinstated cellular NAD<sup>+</sup> levels and SIRT1 activity as well as improved deacetylation of p53 and NF-κB.

NQO1 has many biological activities such as scavenging superoxide anion radicals and stabilizing tumor suppressor p53, which can be the basis for potential intervention in the disease process [40]. However, despite the important role of NQO1, mice lacking NQO1 gene expression showed no detectable phenotype and could not be distinguished from WT mice except that menadione administration increased toxicity compared to WT mice [41]. Interestingly, in this study, we found that the myocardial cell cross-sectional area of NQO1<sup>-/-</sup> mice was significantly increased compared to WT mice (supplemental Fig. S6). This is consistent with a higher LVID during diastole in the NQO1<sup>-/-</sup> mice (Fig. 1A). In addition, the total pool size of NAD (H), i.e. the sum of NAD<sup>+</sup> and NADH, is reduced in NQO1<sup>-/-</sup> mice compared to WT mice. These results suggested that deficiency of NQO1 has caused cardiac stress in absence of ADR.

The role of NAD<sup>+</sup> acts as a rate-limiting co-substrate and a central metabolic cofactor for various enzymes involved in energy metabolism

and cellular homeostasis. Modulation of exogenous NAD<sup>+</sup> biosynthesis shows therapeutic benefits against tissue damage in animal models of ischemia, cardiomyopathy [8], hearing impairment [12], and small intestine injury [17]. Interestingly, intracellular NAD<sup>+</sup>/NADH ratio can be easily controlled by NQO1 that carry out redox reactions by transferring electrons from NADH to its substrates [19,42,43]. Recently, it has been reported that an increase in the NAD<sup>+</sup>/NADH ratio by dunnione, an analog of β-lapachone (a well-known NQO1 substrate), shows beneficial effects on various metabolic syndromes [44], alcoholic ulcers [45], and acute pancreatitis [28].

The cardiac tissue in patients with cancer who receive ADR therapy is very sensitive to oxidative stress, such as ROS, caused by ADR [46]. Correspondingly, our data showed that ADR therapy significantly induced DNA damage in the cardiac tissues through intracellular ROS production. PARP-1, an NAD<sup>+</sup>-dependent DNA repair enzyme and major NAD<sup>+</sup> consumer, is activated by DNA damage under pathological circumstances. Though, excessive activation through severe oxidative DNA damage rapidly reduces intracellular NAD<sup>+</sup> levels, impairing NAD<sup>+</sup>-dependent processes and ultimately leading to cell death [47]. In this study, hyperactivation of PARP-1 was observed in ADR-treated hearts and induced a decrease in cellular NAD<sup>+</sup>/NADH ratio and SIRT1 activity. Likewise, inhibition of PARP activity with ABT-888

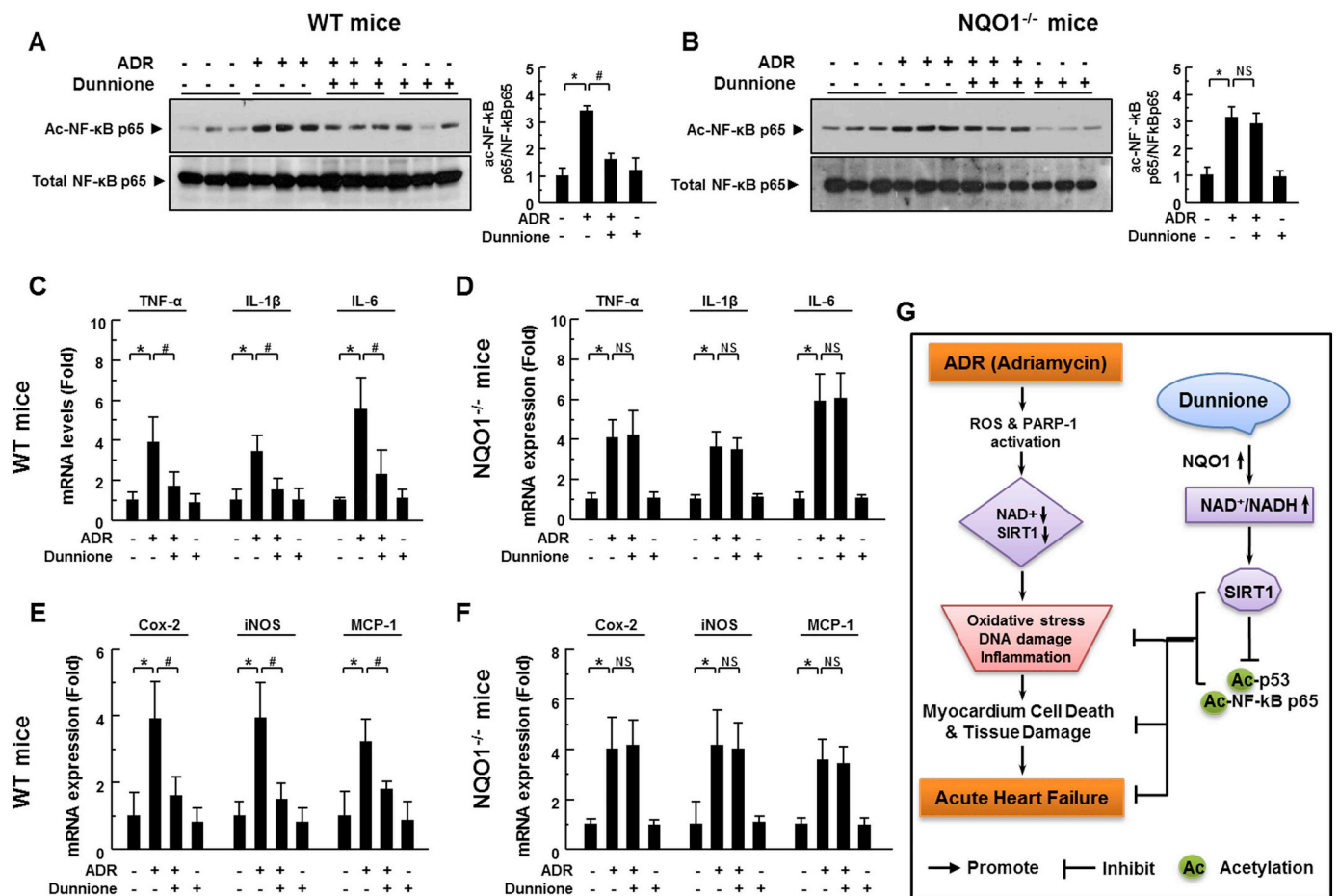


**Fig. 7.** Effect of dunnione on the acetylation of NF-κB p65 and production of pro-inflammatory mediators. A–B. Acetylated NF-κB p65 and total NF-κB p65 levels were determined by western blotting using anti-acetylated NF-κB p65 (K310) and anti-acetylated NF-κB p65 antibodies in WT (A) and NQO1<sup>-/-</sup> (B) mice. Total RNA was isolated from the frozen heart tissues and reverse-transcribed using a transcriptase, and then the resulting cDNA was subjected to real-time PCR according to the manufacturer's protocol. C–D. Quantitative real-time PCR was carried out using primers for the cytokines, TNF-α, IL-1β, and IL-6 in WT (C) and NQO1<sup>-/-</sup> (D) mice. E–F. Quantitative real-time PCR was carried out using primers for the chemokines, COX-2, iNOS, and MCP-1 in WT (E) and NQO1<sup>-/-</sup> (F) mice. G. A working model of the effect of dunnione on ADR-induced cardiomyopathy in mice. \* and # indicate *p* < 0.05 by one-way ANOVA compared with the control (\*) and ADR alone group (#). NS, not significant; (n = 5).

significantly increased the levels of cellular NAD<sup>+</sup>, Sirt1 activity and expression levels of Sirt1, and decreased miR-34a levels in ADR-treated H9c2 cardiomyocytes (Supplemental Fig. S4). Both PARP-1 and SIRT1 can regulate many mutual cell pathways, each of which can affect activity sharing the same intracellular NAD<sup>+</sup> pool [47]. As a result, activation of PARP-1 may significantly affect SIRT1 activity by decreasing NAD<sup>+</sup> bioavailability [48]. This was further demonstrated in a recent study in which the genetic deficiency of PARP-1 or the pharmacological inhibition of PARP-1 activity increased intracellular NAD<sup>+</sup> levels and increased SIRT1 activity [49]. In addition, SIRT1 has a protective role against ADR-induced toxicity [26]. In our study, simultaneous reduction of SIRT1 protein expression and its activity was observed in ADR-treated cardiac tissue. The molecular mechanism by which ADR affects SIRT1 expression is not yet well-known, but the expression of SIRT1 could be regulated by microRNAs (miRNAs). Among them, miR-34a is the first recognized miRNA to regulate cell death and cellular senescence by inhibiting mRNA translation by binding directly to 3'-UTR of SIRT1 [27], and has recently been reported to be an important regulator of cardiac dysfunction [50]. It has also been suggested that miR-34a pharmacological inhibition could be a future therapeutic option for cardioprotection against ADR-induced cardiomyopathy [51]. Of note, activation of p53, especially acetylated p53, is a key upstream regulator for miR-34a [12]. Furthermore, during cellular stress response, the p53 tumor suppressor is an important transcription factor, which regulated

by nuclear SIRT1 through direct interaction with and succeeding deacetylation of p53. The p53 acetylation accelerates sequence-specific DNA-binding following recruitment of other transcription cofactors in nucleus, and thereby improves the transcription of target genes [52], including Ap53-induced gene 3, p53-upregulated modulator of apoptosis, and NADPH activator, all are included in ROS production through apoptosis or mitochondrial dysfunction. The p53 deacetylation through nuclear-localized SIRT1 deactivates transcriptional activity, and suppresses p53-mediated apoptosis and cell growth arrest in response to oxidative stress and DNA damage [53]. In our study, we demonstrated that a significant decrease in Sirt1 activity, which may be associated with a decrease in cellular NAD<sup>+</sup> levels and downregulation of Sirt1 expression, in ADR-induced cardiomyopathy. The decrease in Sirt1 activity permits an increase in p53 acetylation and p53 activity. Activation of p53 increases miR-34a transcription, which in turn suppresses Sirt1 translation by binding directly to 3'-UTR of Sirt1. It is unclear whether a decrease in Sirt1 activity is caused by downregulation of Sirt1 expression or by a decrease in NAD<sup>+</sup> levels, our results suggest that ADR-mediated reduction of Sirt1 expression and NAD<sup>+</sup> levels and subsequent decrease of Sirt1 activity may accelerate the p53-miR-34a pathway through a positive feedback loop. In addition, an increase in NAD<sup>+</sup> levels by dunnione induced SIRT1 activation and reduced heart damage by reducing oxidative stress and DNA damage through down-regulation of p53 deacetylation and miR-34a expression.

It is now well-developed that NF- $\kappa$ B transcription factor plays critical roles in inflammation. NAD<sup>+</sup>-dependent SIRT1 physically interacts with nuclear translocated NF- $\kappa$ B p65 and deacetylates the Lys-310 residue of NF- $\kappa$ B p65 to inhibit the transcriptional activity of NF- $\kappa$ B [12]. In this study, we found that acetylation of NF- $\kappa$ B p65 in the ADR-treated heart tissue was facilitated by reduced SIRT1 activity and expression induced by decreased intracellular NAD<sup>+</sup> and increased miR-34a levels. However, the increase in NAD<sup>+</sup>/NADH ratio by NQO1 using dunnione as a substrate activated SIRT1, and thereby attenuated ADR-induced acetylation of NF- $\kappa$ B p65 as well as production of pro-inflammatory cytokines (TNF- $\alpha$ , IL-1 $\beta$ , and IL-6) and chemokines (COX-2, iNOS, and MCP-1).

In conclusion, we have shown that an increase in cellular NAD<sup>+</sup> can improve ADR-induced cardiac damage and dysfunction through modulation of the PARP-1, SIRT1, p53, and NF- $\kappa$ B signaling pathways (summarized in Fig. 7G). Thus, pharmacological stimulation of NQO1 enzymatic action, which induces an increase of intracellular NAD<sup>+</sup> level, may be a beneficial therapeutic strategy for patients with cancer undergoing ADR chemotherapy.

### Conflicts of interest

The authors declare no potential conflicts of interest.

### Acknowledgements

This work was supported by a National Research Foundation of Korea [NRF] grant funded by the Korean government [MIST]: [No. 2011-0030130].

### Supplementary data

Supplementary data to this article can be found online at <https://doi.org/10.1016/j.jmcc.2018.10.001>.

### References

- [1] R.B. Weiss, The anthracyclines: will we ever find a better doxorubicin? *Semin. Oncol.* 19 (1992) 670–686.
- [2] H. Cortes-Funes, C. Coronado, Role of anthracyclines in the era of targeted therapy, *Cardiovasc. Toxicol.* 7 (2007) 56–60.
- [3] Y. Octavia, C.G. Tocchetti, K.L. Gabrielson, S. Janssens, H.J. Crijns, A.L. Moens, Doxorubicin-induced cardiomyopathy: from molecular mechanisms to therapeutic strategies, *J. Mol. Cell. Cardiol.* 52 (2012) 1213–1225.
- [4] S.E. Lipshultz, V.I. Franco, T.L. Miller, S.D. Colan, S.E. Sallan, Cardiovascular disease in adult survivors of childhood cancer, *Annu. Rev. Med.* 66 (2015) 161–176.
- [5] M. Ghizzoni, H.J. Haisma, H. Maarsingh, F.J. Dekker, Histone acetyltransferases are crucial regulators in NF- $\kappa$ B mediated inflammation, *Drug Discov. Today* 16 (2011) 504–511.
- [6] N. Taira, K. Yoshida, Post-translational modifications of p53 tumor suppressor: determinants of its functional targets, *Histol. Histopathol.* 27 (2012) 437–443.
- [7] S. Oka, C.P. Hsu, J. Sadoshima, Regulation of cell survival and death by pyridine nucleotides, *Circ. Res.* 111 (2012) 611–627.
- [8] P. Belenky, K.L. Bogan, C. Brenner, NAD<sup>+</sup> metabolism in health and disease, *Trends Biochem. Sci.* 32 (2007) 12–19.
- [9] R. Krishnakumar, W.L. Kraus, The PARP side of the nucleus: molecular actions, physiological outcomes, and clinical targets, *Mol. Cell* 39 (2010) 8–24.
- [10] J.B. Pillai, A. Isbatan, S. Imai, M.P. Gupta, Poly(ADP-ribose) polymerase-1-dependent cardiac myocyte cell death during heart failure is mediated by NAD<sup>+</sup> depletion and reduced Sir2alpha deacetylase activity, *J. Biol. Chem.* 280 (2005) 43121–43130.
- [11] X. Li, N. Kazgan, Mammalian sirtuins and energy metabolism, *Int. J. Biol. Sci.* 7 (2011) 575–587.
- [12] H.J. Kim, G.S. Oh, A. Shen, S.B. Lee, S.K. Choe, K.B. Kwon, et al., Augmentation of NAD(+) by NQO1 attenuates cisplatin-mediated hearing impairment, *Cell Death Dis.* 5 (2014) e1292.
- [13] A. Gaikwad, D.J. Long 2nd, J.L. Stringer, A.K. Jaiswal, In vivo role of NAD(P)H:quinone oxidoreductase 1 (NQO1) in the regulation of intracellular redox state and accumulation of abdominal adipose tissue, *J. Biol. Chem.* 276 (2001) 22559–22564.
- [14] J.H. Hwang, D.W. Kim, E.J. Jo, Y.K. Kim, Y.S. Jo, J.H. Park, et al., Pharmacological stimulation of NADH oxidation ameliorates obesity and related phenotypes in mice, *Diabetes* 58 (2009) 965–974.
- [15] R.H. Haefeli, M. Erb, A.C. Gemperli, D. Robay, I. Courdier Fruh, C. Anklin, et al., NQO1-dependent redox cycling of idebenone: effects on cellular redox potential and energy levels, *PLoS One* 6 (2011) e17963.
- [16] X. Huang, Y. Dong, E.A. Bey, J.A. Kilgore, J.S. Bair, L.S. Li, et al., An NQO1 substrate with potent antitumor activity that selectively kills by PARP1-induced programmed necrosis, *Cancer Res.* 72 (2012) 3038–3047.
- [17] A. Pandit, H.J. Kim, G.S. Oh, A. Shen, S.B. Lee, D. Khadka, et al., Dunnione ameliorates cisplatin-induced small intestinal damage by modulating NAD(+) metabolism, *Biochem. Biophys. Res. Commun.* 467 (2015) 697–703.
- [18] S.W. Standage, R.L. Waworuntu, M.A. Delaney, S.M. Maskal, B.G. Bennion, J.S. Duffield, et al., Nonhematopoietic peroxisome proliferator-activated receptor-alpha protects against cardiac injury and enhances survival in experimental polymicrobial sepsis, *Crit. Care Med.* 44 (2016) e594–e603.
- [19] Y.H. Kim, J.H. Hwang, J.R. Noh, G.T. Gang, S. Tadi, Y.H. Yim, et al., Prevention of salt-induced renal injury by activation of NAD(P)H:quinone oxidoreductase 1, associated with NADPH oxidase, *Free Radic. Biol. Med.* 52 (2012) 880–888.
- [20] E.M. Mantawy, A. Esmat, W.M. El-Bakly, R.A. Salah Eldin, E. El-Demerdash, Mechanistic clues to the protective effect of chrysin against doxorubicin-induced cardiomyopathy: plausible roles of p53, MAPK and AKT pathways, *Sci. Rep.* 7 (2017) 4795.
- [21] O.J. Arola, A. Saraste, K. Pulkki, M. Kallajoki, M. Parvinen, L.M. Voipio-Pulkki, Acute doxorubicin cardiotoxicity involves cardiomyocyte apoptosis, *Cancer Res.* 60 (2000) 1789–1792.
- [22] U. Forstermann, Oxidative stress in vascular disease: causes, defense mechanisms and potential therapies, *Nat. Clin. Pract. Cardiovasc. Med.* 5 (2008) 338–349.
- [23] Y.L. Lyu, J.E. Kerrigan, C.P. Lin, A.M. Azarova, Y.C. Tsai, Y. Ban, et al., Topoisomerase IIbeta mediated DNA double-strand breaks: implications in doxorubicin cardiotoxicity and prevention by dexrazoxane, *Cancer Res.* 67 (2007) 8839–8846.
- [24] Y. Wang, N.S. Kim, J.F. Haince, H.C. Kang, K.K. David, S.A. Andrabi, et al., Poly(ADP-ribose) (PAR) binding to apoptosis-inducing factor is critical for PAR polymerase-1-dependent cell death (parthanatos), *Sci. Signal.* 4 (2011) ra20.
- [25] K.S. Seo, J.H. Park, J.Y. Heo, K. Jing, J. Han, K.N. Min, et al., SIRT2 regulates tumor hypoxia response by promoting HIF-1alpha hydroxylation, *Oncogene* 34 (2015) 1354–1362.
- [26] S. Wang, Y. Wang, Z. Zhang, Q. Liu, J. Gu, Cardioprotective effects of fibroblast growth factor 21 against doxorubicin-induced toxicity via the SIRT1/LKB1/AMPK pathway, *Cell Death Dis.* 8 (2017) e3018.
- [27] M. Yamakuchi, M. Ferlito, C.J. Lowenstein, miR-34a repression of SIRT1 regulates apoptosis, *Proc. Natl. Acad. Sci. U. S. A.* 105 (2008) 13421–13426.
- [28] A. Shen, H.J. Kim, G.S. Oh, S.B. Lee, S.H. Lee, A. Pandit, et al., NAD<sup>+</sup> augmentation ameliorates acute pancreatitis through regulation of inflammasome signalling, *Sci. Rep.* 7 (2017) 3006.
- [29] A. De Angelis, E. Piegari, D. Cappetta, R. Russo, G. Esposito, L.P. Ciuffreda, et al., SIRT1 activation rescues doxorubicin-induced loss of functional competence of human cardiac progenitor cells, *Int. J. Cardiol.* 189 (2015) 30–44.
- [30] S. Cao, X. Zhang, J.P. Edwards, D.M. Mosser, NF- $\kappa$ B1 (p50) homodimers differentially regulate pro- and anti-inflammatory cytokines in macrophages, *J. Biol. Chem.* 281 (2006) 26041–26050.
- [31] J. Das, J. Ghosh, P. Manna, P.C. Sil, Taurine suppresses doxorubicin-triggered oxidative stress and cardiac apoptosis in rat via up-regulation of PI3-K/Akt and inhibition of p53, p38-JNK, *Biochem. Pharmacol.* 81 (2011) 891–909.
- [32] J. Niu, A. Azfer, K. Wang, X. Wang, P.E. Kolattukudy, Cardiac-targeted expression of soluble fas attenuates doxorubicin-induced cardiotoxicity in mice, *J. Pharmacol. Exp. Ther.* 328 (2009) 740–748.
- [33] A.L. Ferreira, L.S. Matsubara, B.B. Matsubara, Anthracycline-induced cardiotoxicity, *Cardiovasc. Hematol. Agents Med. Chem.* 6 (2008) 278–281.
- [34] T. Eschenhagen, T. Force, M.S. Ewer, G.W. de Keulenaer, T.M. Suter, S.D. Anker, et al., Cardiovascular side effects of cancer therapies: a position statement from the Heart Failure Association of the European Society of Cardiology, *Eur. J. Heart Fail.* 13 (2011) 1–10.
- [35] P.K. Singal, T. Li, D. Kumar, I. Danelisen, N. Iliskovic, Adriamycin-induced heart failure: mechanism and modulation, *Mol. Cell. Biochem.* 207 (2000) 77–86.
- [36] G. Minotti, P. Menna, E. Salvatorelli, G. Cairo, L. Gianni, Anthracyclines: molecular advances and pharmacologic developments in antitumor activity and cardiotoxicity, *Pharmacol. Rev.* 56 (2004) 185–229.
- [37] M. Yoshida, I. Shiojima, H. Ikeda, I. Komuro, Chronic doxorubicin cardiotoxicity is mediated by oxidative DNA damage-ATM-p53-apoptosis pathway and attenuated by pitavastatin through the inhibition of Rac1 activity, *J. Mol. Cell. Cardiol.* 47 (2009) 698–705.
- [38] D.S. Kim, E.R. Woo, S.W. Chae, K.C. Ha, G.H. Lee, S.T. Hong, et al., Plantainoside D protects adriamycin-induced apoptosis in H9c2 cardiac muscle cells via the inhibition of ROS generation and NF- $\kappa$ B activation, *Life Sci.* 80 (2007) 314–323.
- [39] M.P. Cole, J. Tangpong, T.D. Oberley, L. Chaiswing, K.K. Kinningham, D.K. St Clair, Nuclear interaction between ADR-induced p65 and p53 mediates cardiac injury in iNOS (-/-) mice, *PLoS One* 9 (2014) e89251.
- [40] S. Faubel, E.C. Lewis, L. Reznikov, D. Ljubanovic, T.S. Hoke, H. Somers, et al., Cisplatin-induced acute renal failure is associated with an increase in the cytokines interleukin (IL)-1beta, IL-18, IL-6, and neutrophil infiltration in the kidney, *J. Pharmacol. Exp. Ther.* 322 (2007) 8–15.
- [41] V. Radjendirane, P. Joseph, Y.H. Lee, S. Kimura, A.J. Klein-Szanto, F.J. Gonzalez, et al., Disruption of the DT diaphorase (NQO1) gene in mice leads to increased menadione toxicity, *J. Biol. Chem.* 273 (1998) 7382–7389.
- [42] S.Y. Kim, N.H. Jeoung, C.J. Oh, Y.K. Choi, H.J. Lee, H.J. Kim, et al., Activation of NAD(P)H:quinone oxidoreductase 1 prevents arterial restenosis by suppressing vascular smooth muscle cell proliferation, *Circ. Res.* 104 (2009) 842–850.
- [43] J.S. Lee, A.H. Park, S.H. Lee, J.H. Kim, S.J. Yang, Y.I. Yeom, et al., Beta-lapachone, a

- modulator of NAD metabolism, prevents health declines in aged mice, *PLoS One* 7 (2012) e47122.
- [44] R. Krishnakumar, W.L. Kraus, The PARP side of the nucleus: molecular actions, physiological outcomes, and clinical targets, *Mol. Cell* 39 (2010) 8–24.
- [45] I.G. Jo, D. Park, J. Kyung, D. Kim, J. Cai, J. Kim, et al., Inhibitory effects of a beta-dunnione compound MB12662 on gastric secretion and ulcers, *Lab. Anim. Res.* 29 (2013) 178–181.
- [46] B.D. Sahu, J.M. Kumar, M. Kuncha, R.M. Borkar, R. Srinivas, R. Sistla, Baicalein alleviates doxorubicin-induced cardiotoxicity via suppression of myocardial oxidative stress and apoptosis in mice, *Life Sci.* 144 (2016) 8–18.
- [47] J.B. Pillai, A. Isbatan, Imai S-I, M.P. Gupta, Poly (ADP-ribose) polymerase-1-dependent cardiac myocyte cell death during heart failure is mediated by NAD<sup>+</sup> depletion and reduced Sir2 $\alpha$  deacetylase activity, *J. Biol. Chem.* 280 (2005) 43121–43130.
- [48] C. Canto, J. Auwerx, NAD<sup>+</sup> as a signaling molecule modulating metabolism, *Cold Spring Harb. Symp. Quant. Biol.* 76 (2011) 291–298.
- [49] P. Bai, C. Canto, H. Oudart, A. Brunyanszki, Y. Cen, C. Thomas, et al., PARP-1 inhibition increases mitochondrial metabolism through SIRT1 activation, *Cell Metab.* 13 (2011) 461–468.
- [50] B.C. Bernardo, X.M. Gao, C.E. Winbanks, E.J. Boey, Y.K. Tham, H. Kiriazis, et al., Therapeutic inhibition of the miR-34 family attenuates pathological cardiac remodeling and improves heart function, *Proc. Natl. Acad. Sci. U. S. A.* 109 (2012) 17615–17620.
- [51] E. Piegari, R. Russo, D. Cappetta, G. Esposito, K. Urbanek, C. Dell'Aversana, et al., MicroRNA-34a regulates doxorubicin-induced cardiotoxicity in rat, *Oncotarget* 7 (2016) 62312–62326.
- [52] W. Gu, R.G. Roeder, Activation of p53 sequence-specific DNA binding by acetylation of the p53 C-terminal domain, *Cell* 90 (1997) 595–606.
- [53] C.L. Brooks, W. Gu, The impact of acetylation and deacetylation on the p53 pathway, *Protein Cell.* 2 (2011) 456–462.